21, rue d'Artois, F-75008 PARIS
http : //www.cigre.org

CIGRE US National Committee
2019 Grid of the Future Symposium

# Site Acceptance Test for Solar PV System of Bronzeville Community Microgrid

**A. MAJZOOBI, M. BAZRAFSHAN, A. KHODAEI**
**University of Denver**
**USA**

**N. GURUNG, S. KOTHANDARAMAN, H. CHEN, L. ZHANG, A. V. GUERRA**
**ComEd**
**USA**

## SUMMARY

With the increase in penetration of variable renewable energy generation, power systems encounter new challenges in supply-load balance. Microgrids, as small-scale power systems with local control and islanding capability, provide a viable solution for this challenge through leveraging their inherent flexibility. ComEd is developing an urban community microgrid in the Bronzeville neighborhood of Chicago, called Bronzeville Community Microgrid (BCM) that will investigate this challenge in a practical setting. One of the main goals of this project is to capture solar generation variability via a PV-battery integration. By coordinating solar PV and battery energy storage, through a master controller and smart inverters, the integrated PV-battery system is further seen as a dispatchable energy resource with grid-forming functionalities. This paper presents analyses pertaining to site acceptance test (SAT) for the solar PV system. The SAT is required to ensure that the installed microgrid operates smoothly in different conditions, and, moreover, that the protection and communication units are capable of controlling the PV and battery systems perfectly.

## KEYWORDS

Battery Energy Storage, Microgrid, Photovoltaic, Site Acceptance Test

This material is based upon work supported by the U.S. Department of Energy's Office of Energy Efficiency and Renewable Energy (EERE) under Solar Energy Technologies Office (SETO) Agreement Number EE0007166.
amin.khodaei@du.edu

## 1. INTRODUCTION

Renewable energy is recognized globally as a growing source of electricity generation. Solar photovoltaic (PV) and wind have had a noticeable growth as two main renewable energy resources in the recent years. Solar PV global capacity in 2018 reached 505 GW, compared with 40 GW in 2010 [1]. Similarly, wind power global capacity in 2018 was 591 GW, three times its capacity in 2010 [1]. High penetration of renewable generation has resulted in new challenges in power systems, mainly due to their inherent variability [2-4]. Leveraging available flexibility of microgrid has been introduced as a local solution for this challenge [5-8]. The microgrid's master controller manages the dispatchable energy resources, such as distributed generations (DGs) and energy storage, to capture the variability of renewable generation. Specifically, integration of solar and energy storage has increasingly attracted attention in recent years as a practical solution for this challenge [9,10].

ComEd, the electric utility company serving approximately 4 million customers in northern Illinois, is developing a community microgrid in the South Side Chicago neighborhood of Bronzeville, to address the inherent fluctuations of solar PV generation by utilizing battery energy storage system (BESS) and smart inverters [11]. The Bronzeville Community Microgrid (BCM) is adjacent to the Illinois Institute of Technology (IIT) campus microgrid, which together create the world's first microgrid cluster. BCM embeds a 587 kW distributed rooftop PV system, grouped in two parts; a Northern PV group and a Southern PV group. Each group consists of several smart inverters, located on the roof of the various buildings in each group. There are eight and nine inverters in the north and south groups, respectively. A real time automation controller (RTAC) device is used to aggregate the multiple PV inverters in each group. The rooftop PV systems are communicating with an aggregator to capture all PV measurements. In addition, the RTAC provides the interface for controlling and complying with the control sequence associated with PV inverters. The BESS unit is a utility-owned front-of-meter 500 kW/2 MWh system. Fig. 1 depicts the one-line diagram of BCM.

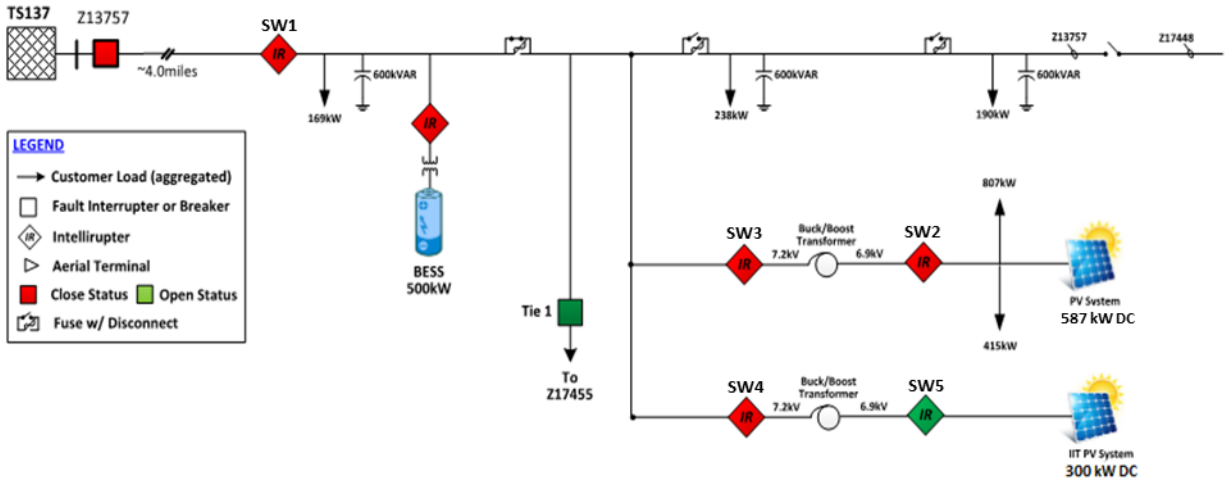


Figure 1. One-line diagram of the BCM.

To ensure that all equipment and parts of BCM, including the communication and control links, have been installed and operated properly, a series of site acceptance tests (SATs) should be conducted on BESS and PV systems. The key control features of the PV system that should be assessed in SAT are:

- PV real power control (curtailment) with remote signal
- Dynamic reactive power setpoint adjustment with remote signal
- Power factor adjustment
- Ramp rate control with adjustable settings
- Volt-VAR control, using voltage droop with adjustable settings
- Nighttime reactive power compensation

The tests are performed using a RTAC, which emulates the SCADA system, located in the ComEd PV control and monitoring cabinet. Data from the tests are automatically captured by a data logger. The rest of this paper presents the analysis of results of three tests that comprise part of the SAT for the PV system. Sections 2, 3, and 4 respectively cover the real power control test, the power factor adjustment test, and ramp rate control test. The paper is concluded in Section 5.

## 2. REAL POWER CONTROL TEST

The main purpose of this test is to verify remote control and curtailment of PV system, using real power setpoint sent to RTAC for each group. Figure 2 depicts the values of real power setpoint and real power measurement (3-phase) for both groups 1 and 2. In this case, the setpoint of real power for the inverter is determined by the real power set point percent command.

In group 1, before sending any command, the real power output of inverters is around 125 kW. It should be noted that this is the maximum available power for that time and is obviously less than group 1 inverters size (400 kW) due to solar conditions. When the real power setpoint is commanded to be 100% at t=10s, the real power measurements from inverters drop momentarily but return to the original value. At t=35s the real power setpoint is commanded to be 20% and the real power measurements from inverters drop to around 75 kW, which is approximately 20% of the inverter size. This is realizable because the irradiance supports 20% of 400 kW for that time but does not support 100% of 400 kW. At t=63s, the real power setpoint is changed to 60% and subsequently the real power measurements from inverters returns to around 125 kW, since 60% of 400 kW is greater than 125 kW, which is the maximum available solar generation from the inverters for that day based on the irradiance. The results demonstrate a similar pattern for PV system group 2. Therefore, the results of this test clearly show that real power closely follows the defined setpoints and the controller operates properly.

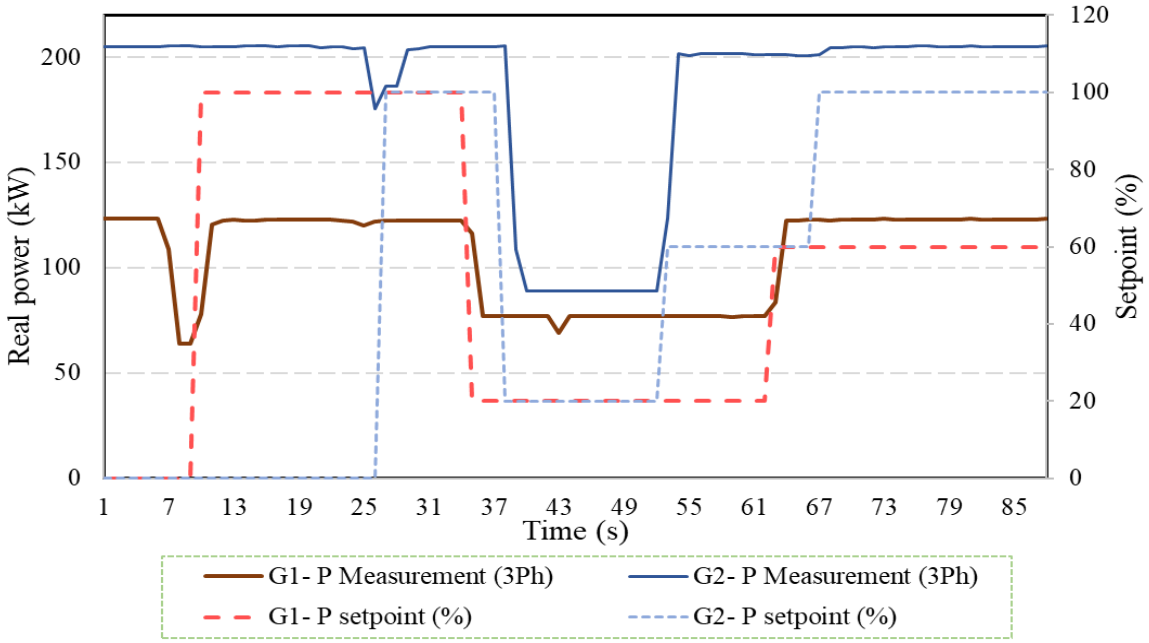


Figure 2, Real power control test results.

## 3. POWER FACTOR ADJUSTMENT TEST

The purpose of this test is to observe that the power factor output of the PV inverter can be controlled or maintained at a desired value. In this test, the control mode is set to "Power Factor Mode" with Q priority. The response of the inverter to changes in power factor setpoint as well as changes in real and reactive power setpoint are verified. Figure 3 depicts the setpoints and measured values for real and reactive power for group 1 solar system. We should note that in this figure, positive and negative values of reactive power respectively imply *consumption* and *injection.* Also, Figure 4 shows the relevant calculated power factor and power factor setpoint. It should be mentioned that the calculated power factor uses the real and reactive power measurements. Indeed, given $p$ and $q$, respectively, as PV inverter real and reactive power measurements, the power factor is

$$pf = sign(q) * \frac{p}{\sqrt[2]{p^2 + q^2}} \quad \#(1)$$

In the above equation $sign(0)$ is interpreted to be 1. The expression $sign(q)$ is included in equation (1) to allow accommodation of both leading and lagging power factors in the same figure. A positive $pf$ from (1) implies a lagging power factor and a negative $pf$ from (1) implies a leading power factor. In the explanation that follows, for real and reactive power quantities please view Figure 3 and for power factor quantities please view Figure 4.

As Figure 3 shows, the real power setpoint is initially set to 50% of $P_{max}$, and the generation is 108 kW. As mentioned in Section 2.1, this output is due to solar conditions. Moreover, the power factor is initially set to 0.9 leading, and consequently the reactive power *consumption* will be 54 kVAR. At t=18s, real power setpoint is set to 10% of $P_{max}$, resulting in generation of 40 kW. As a result of change in real power, the reactive power generation decreases to 18.5 kVAR to keep the power factor at 0.9 leading. It should be noted that there is no change in reactive power setpoint at this time, but since the control mode is set to power factor mode, the reactive power is changed to keep power factor at its setpoint.

As Figure 4 shows, the power factor setpoint is changed to 0.9 lagging at t=53s. According to Figure 3, the real and reactive power setpoints at this time are fixed, but the inverters started *injecting* 15.5 kVAR to follow the power factor setpoint. Furthermore, to check the priority of power factor setpoint, the setpoint of reactive power is changed to 50% at t=115s, while the power factor setpoint is still 0.9 lagging. Although the reactive power setpoint is increased at this time, there is no change in reactive power to keep the power factor at the commanded value. At t=140s, the power factor setpoint is changed to 0.8 leading and the inverters start *consuming* 28 kVAR, while there is no change in reactive power setpoint. The real power setpoint is further changed to 100% of $P_{max}$ at t=170s. As a result, the real power is increased to about 106 kW (again, not reaching the full capacity due to solar conditions) and, correspondingly, the reactive power consumption increases to maintain the power factor setpoint, i.e. 0.8 leading. Changing the power factor setpoint to 0.8 lagging, at t=204s, leads to 65 kVAR reactive power injection, again with no change in real power.

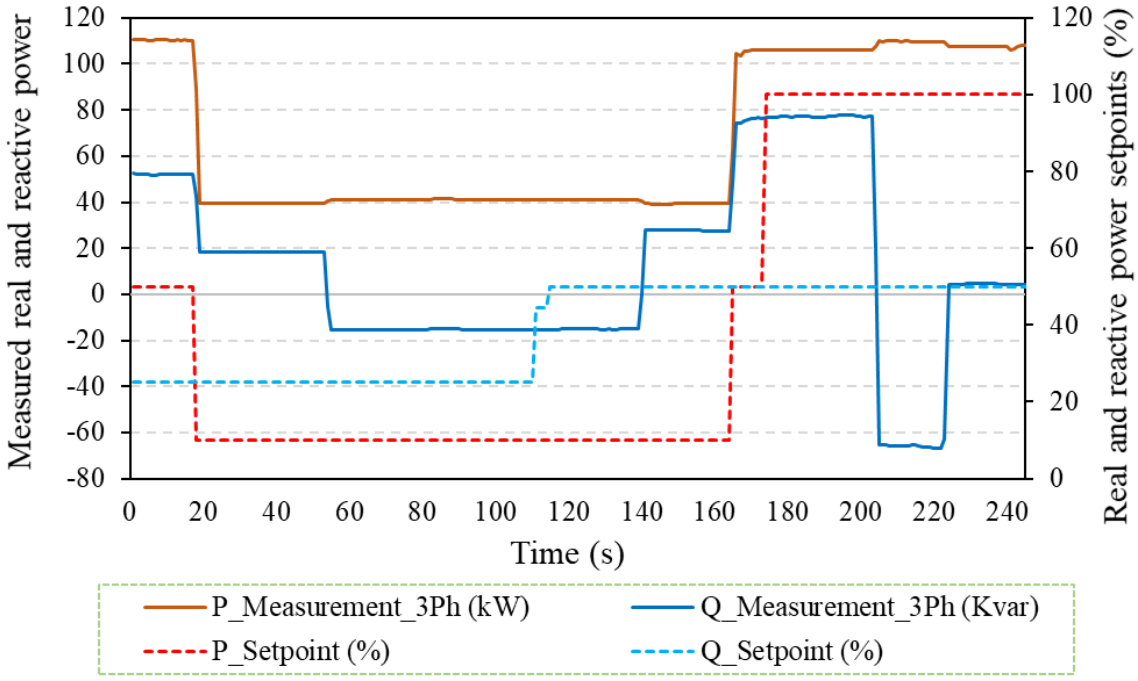


Figure 3. Real and reactive powers in power factor adjustment test for group 1 solar system.

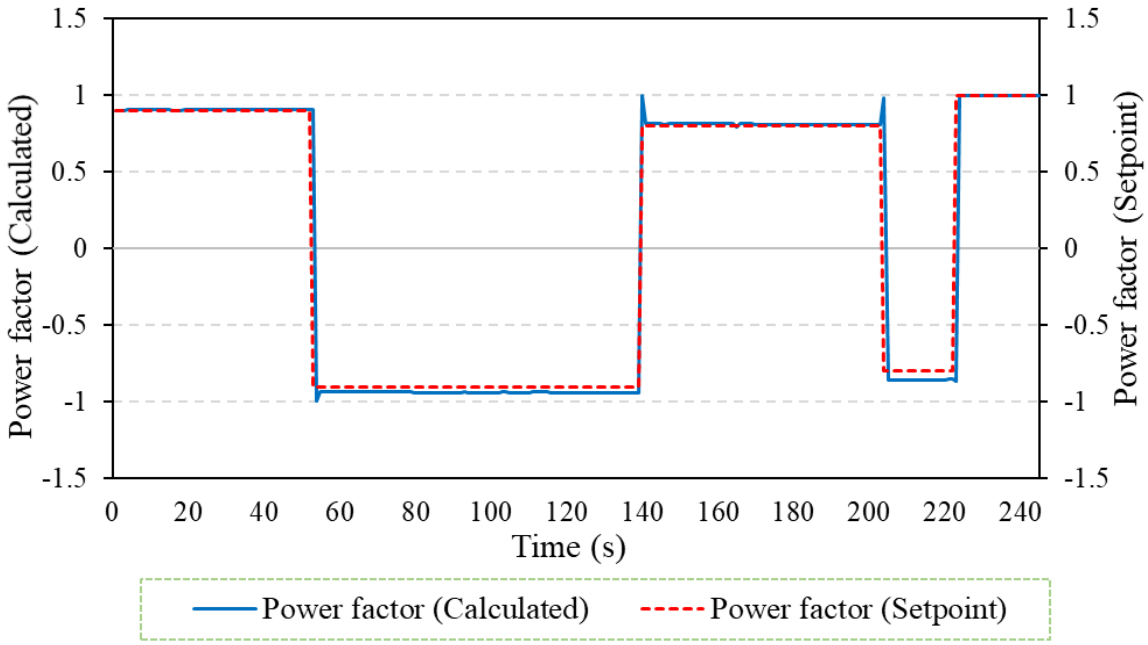


Figure 4. Power factor results in power factor adjustment test for group 1 solar system.

## 4. RAMP RATE CONTROL TEST

The inverter provides the ability to adjust the maximum up and down ramp rates. This test is designed to verify this ability of inverter and the response of the inverters to change in real power at different ramp rate settings. The test results are plotted in Figure 5.

In this test, the control mode is set to "P in percentage of $P_{max}$" and it is initially set to 10% of $P_{max}$ for group 1. In addition, the ramp rate of the inverter is set to the minimum adjustable setting which is 10% of $P_{max}$ per second. In this condition, the real power setpoint is changed to 100% of $P_{max}$ for group 1 at t=4s. Accordingly, as Figure 5 shows, the real power generation of group 1 takes about 10 seconds to reach its maximum as the solar conditions at the time of test permits.

To test another ramp rate setting, the ramp rate limit is commanded to be the maximum adjustable setting, i.e. 100% of $P_{max}$ per second. The P setpoint is set to 100% of $P_{max}$, and consequently the real powers of group 1 reach 91 kW in less than 5s. The value of 91 kW is the maximum generation based on the solar conditions at the time of test and the value of 5 seconds is the resolution of the datalogger. Therefore, the test results imply the real power gradient is able to follow different commanded ramp rates for group 1. A similar situation is indicated for group 2 inverters in Figure 5.

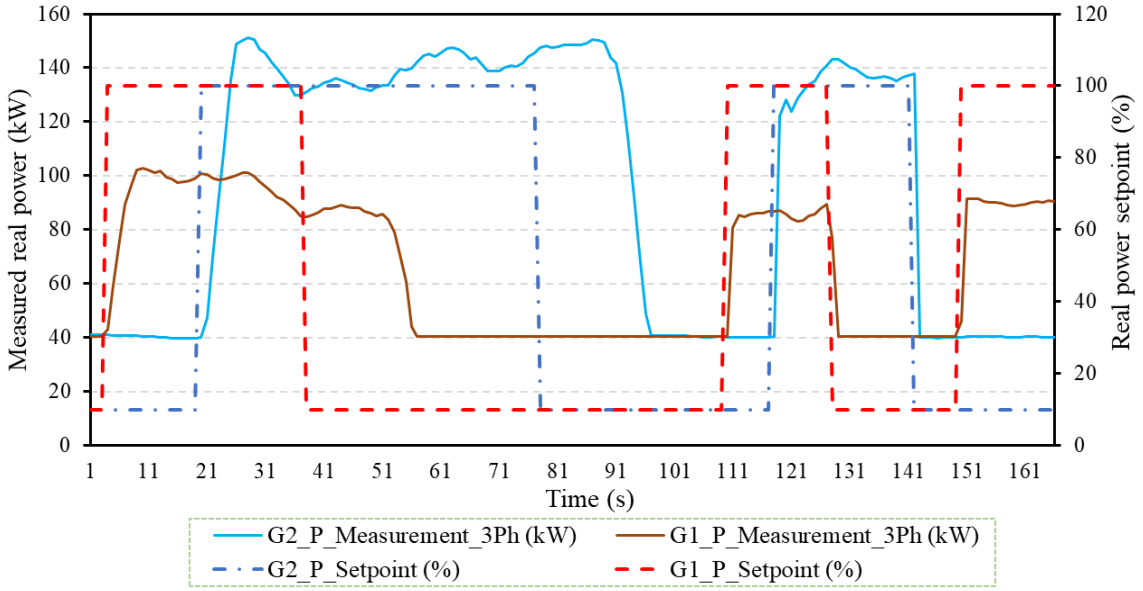


Figure 5. Measured real power in ramp rate control test.

## 5. CONCLUSIONS

This paper presented important phases of the PV system SAT and further analyzed the tests results. According to the test results, real power and the power factor closely follow their relevant setpoints and expected trend, which clearly verify the proper performance of the solar PV system and smart inverters. The growing penetration of solar PV generation in distribution systems calls for practical tests on the technology, particularly when integrated with a battery energy storage within a microgrid, as was studied in ComEd's project and explained in this paper.

## BIBLIOGRAPHY

[1] REN21, "Renewables 2019: global status report," 2019.

[2] P. Ferraro, E. Crisostomi, M. Raugi and F. Milano, "Analysis of the Impact of Microgrid Penetration on Power System Dynamics," (IEEE Transactions on Power Systems, volume 32, number 5, September 2017, pages 4101-4109).

[3] J.A. Peças Lopes, N. Hatziargyriou, J. Mutale, P. Djapic, N. Jenkins, "Integrating distributed generation into electric power systems: A review of drivers, challenges and opportunities" (Electric Power Systems Research, volume 77, number 9, July 2007, Pages 1189-1203).

[4] S. Eftekharnejad, V. Vittal, G. T. Heydt, B. Keel and J. Loehr, "Impact of increased penetration of photovoltaic generation on power systems" (IEEE Transactions on Power Systems, volume 28, number 2, May 2013, pages 893-901).

[5] H. Bevrani, "Microgrid control: A solution for penetration of renewable power" (2017 International Conference on Green Energy and Applications (ICGEA), Singapore, March 2017, pages 46-51).

[6] S. Bifaretti, S. Cordiner, V. Mulone, V. Rocco, J.L. Rossi, F. Spagnolo, "Grid-connected Microgrids to Support Renewable Energy Sources Penetration" (Energy Procedia, volume 105, May 2017, Pages 2910-2915).

[7] A. Majzoobi, A. Khodaei, and S. Bahramirad, "Capturing Distribution Grid-Integrated Solar Variability and Uncertainty Using Microgrids" (IEEE Power and Energy Society General Meeting, Chicago, IL, July 2017, pages 1–5).
[8] A. Majzoobi, A. Khodaei, S. Bahramirad, and M. H. J. Bollen, "Capturing the variabilities of distribution network net-load via available flexibility of microgrids" (Grid of the Future Symposium (CIGRE), Philadelphia, PA, 2016).
[9] C. A. Hill, M. C. Such, D. Chen, J. Gonzalez and W. M. Grady, "Battery Energy Storage for Enabling Integration of Distributed Solar Power Generation" *(*IEEE Transactions on Smart Grid, volume 3, number 2, June 2012, pages 850-857).
[10] H. R. Teymour, D. Sutanto, K. M. Muttaqi and P. Ciufo, "Solar PV and Battery Storage Integration using a New Configuration of a Three-Level NPC Inverter With Advanced Control Strategy," *(*IEEE Transactions on Energy Conversion, volume 29, number 2, June 2014, pages 354-365).
[11] ComEd, "Bronzeville Community of The Future," [Online]. Available: https://bronzevillecommunityofthefuture.com/project-microgrid/. [Accessed 13 July 2019].